Validity of Phase Space Theory for Atom−Diatom Insertion Reactions†

P. Larrégaray,* L. Bonnet, and J.-C. Rayez

Laboratoire de Physico-Chimie Moléculaire, UMR5803, Université Bordeaux1-CNRS, 33405 Talence Cedex, France

Received: July 12, 2005; In Final Form: September 6, 2005

Phase space theory (PST) is applied to the calculation of state-resolved integral and differential cross sections for the complex-forming atom−diatom insertion reactions $A + H_2 \rightarrow AH_2 \rightarrow AH + H$ with A = C(^{1}D), S(^{1}D), O(^{1}D), and N(^{2}D). In the asymptotic channels, vibration motion is quantized while rotation and translation motions are treated classically. The approach is compared to exact quantum scattering calculations and quantum statistical models. Given the simplicity of PST, the agreement with the previous much more refined treatments is very satisfying. Although PST is a well-established theory, this work is, to our knowledge, the first such systematic comparison of its predictions with accurate quantum scattering and quantum statistical calculations.

1. Introduction

Atom−diatom insertion reactions have recently attracted a lot of interest,[1,2] namely, the prototypical processes $A + H_2 \rightarrow AH_2 \rightarrow AH + H$ with A = C(^{1}D), N(^{2}D), O(^{1}D), or S(^{1}D). In contrast with the extensively studied direct abstraction mechanisms (e.g. $H + H_2$, $F + H_2$, or $Cl + H_2$), these reactions proceed via a stable AH_2 intermediate complex associated with a deep potential energy well. From the experimental point of view, state-resolved integral and differential cross sections (respectively ICS and DCS) have been measured.[3−6] From the theoretical point of view, tremendous advances in exact time-independent quantum scattering calculations have allowed the prediction of the previous observables with an excellent level of accuracy.[7−10] Besides, approximate time-dependent quantum scattering approaches have also been examined.[11−15] However, both types of quantum dynamics simulations are extremely difficult to implement routinely because of the huge number of bound and low-lying resonance states of the collision complex to account for. Nevertheless, for weak collision energies (lower than 0.2 eV), the existence of sharp resonances in the computed reaction probabilities have suggested that the AH_2 intermediate complex may live long enough for its formation and decay into reactant and product channels to be treatable statistically. The long lifetime of the intermediate complex has also been evidenced by quasi-classical trajectory[16] and quantum mechanical calculations.[17] In other words, the strength of couplings existing between the AH_2 internal degrees of freedom, in the region of the well (strong coupling region, SCR), may be responsible for fast randomization of energy among the complex vibrational modes. Consequently, within the framework of classical mechanics, the distribution of the SCR phase space states may be regarded as microcanonical.[18]

Following this idea, Rackham et al. developed a so-called coupled-channel statistical model (CCS)[19] in which (i) intermediate complex states are assumed to be distributed statistically and (ii) reactant and product channels dynamics are treated within a time-independent quantum formalism using the ab initio potential energy surfaces (PESs).[20−23] This model, which has been tested for the four above-mentioned processes,[24] has now been extended to take into account multiple electronic states.[25] Similarly, Lin et al. proposed a wave packet based statistical model (WPS)[26] differing from the CCS one in that asymptotic channels dynamics are computed within a time-dependent quantum approach. The WPS model has been illustrated by the study of the processes involving C(^{1}D) and S(^{1}D).[12,26,27] Both the CCS and WPS models are much more convenient to implement than the exact quantum scattering calculations since, within the statistical assumption, formation and decay of the intermediate complex can be regarded as independent events which only require inelastic collision calculations in both entrance and exit channels. These "exact" statistical models have predicted state-resolved integral and differential cross sections in remarkable agreement with their quantum and experimental counterparts. Hence, the statistical assumption on which they rely seems to be justified.

In addition to these statistical approaches, quasi classical trajectory simulations (QCT)[4,5,16,21,28,29] have led to a fair prediction of state-resolved ICSs, provided that product internal vibration motion is properly quantized.[30,31] These results imply that ro-translation dynamics can reasonably be considered as classical in the asymptotic channels. Conversely, these simulations have not been able to accurately reproduce the sharp forward/backward peaks existing in the state-resolved and total DCSs. This strong polarization has been attributed to tunneling through entrance and exit centrifugal barriers[4,24] and, thus, is not accounted for in the QCT method.

In summary, the previous studies on the atom−diatom insertion reactions tend to show that (i) the AH_2 species is sufficiently long-lived for the statistical assumption to be valid and (ii) rotation and translation dynamics can be treated classically but internal vibration must be appropriately quantized.

Moreover, for the reactions involving O(^{1}D), S(^{1}D), and C(^{1}D), reactant and product channels are barrierless. Therefore, given the collision energies employed in the above studies, entrance and exit channel dynamics should be governed by long-range isotropic van der Waals forces. As a consequence, the phase space theory[32−36] (PST) should apply. Briefly, in PST, complex formation cross section is estimated via the classical Langevin capture model[37] and the probability of formation of

† Part of the special issue "William Hase Festschrift".

* Corresponding author. E-mail: p.larregaray@lpcm.u-bordeaux1.fr.

10.1021/jp053822x CCC: $33.50
Published on Web 10/18/2005

any given product from the intermediate complex is proportional to the ratio of the phase space available to that product divided by the total phase space consistent with conservation of energy and total angular momentum.

Conversely, a small potential energy barrier and a strong anisotropy characterize the $N(^2D) + H_2$ reactant channel so that Langevin capture theory cannot apply to determine the NH_2 complex formation cross section. To circumvent this limitation, we recently proposed a model[38] going beyond the angular-dependent line-of-center (ADLOC) model.[39] This approach, referred to in the following as the post-ADLOC model, takes into account reorientation of the H_2 molecule during reactant approach and tunneling through the entrance barrier.

In this study, we implement a semiclassical version of phase space theory (labeled PST in the following) in which internal vibration motion is quantized and tunneling through reactant and product potential/centrifugal barriers is approximately accounted for. This approach, presented in section 2, is applied to the reactions of $O(^1D)$, $S(^1D)$, and $C(^1D)$ with H_2. Besides, PST is slightly modified in order to accurately estimate the intermediate complex formation cross section for the $N + H_2$ process. For the four processes, results are compared with exact quantum calculations and the previously proposed exact statistical models in section 3. Section 4 concludes.

2. Theory

The complex forming triatomic reactions under consideration are of the type

$$A + H_2 \rightarrow AH_2 \rightarrow A + H_2(v, j) \quad \text{(reactant channel R)} \quad (1a)$$

$$\rightarrow AH(v', j') + H \quad \text{(product channel P)} \quad (1b)$$

As H_2 is a homonuclear diatom, product channel P is 2-fold degenerate. However, the forthcoming developments can be trivially extended to the general case.[40] To implement PST, the following set of assumptions is considered:

(1) Since the reactant diatom rotational angular momentum is usually small in molecular beam experiments[1,2] (a few $\hbar$ units), the H_2 diatom is initially considered in its ro-vibrational ground state (v=0, j=0).

(2) Dynamics in reactant and product channels is supposed to be governed by isotropic van der Waals forces. This standard approximation is typically valid for barrierless channels in which the fragment relative energy is not too important.[40] Accordingly, internal vibration, rotation, and translation motions are uncoupled. The interaction potential energy between fragments is here approximated by[41]

$$V(R) = -\frac{C_6}{R^6} \quad (2)$$

where R is the distance between the atom and the diatom center-of-mass. In reactant channels, only dispersion forces are considered so that the C_6 term is calculated using the Slater−Kirkwood formula,[42]

$$C_6 = C_6^{\text{disp}} = \frac{3}{2}\frac{e\hbar}{\sqrt{m_e}}\left(\frac{\alpha_A\alpha_{H_2}}{\sqrt{\frac{\alpha_A}{n_A}} + \sqrt{\frac{\alpha_{H_2}}{n_{H_2}}}}\right) \quad (3)$$

where α_i and n_i are respectively the polarizability and the number of electrons in the highest occupied molecular orbital (HOMO) for the species i (i = A, H_2), e is the electron charge, and m_e is the electron mass. For product channels, in addition to the dispersion term, the interaction between the AH permanent dipole and the induced dipole of H is also accounted for so that

$$C_6 = C_6^{\text{disp}} + C_6^{\text{ind}} \quad (4)$$

The inductive contribution, C_6^{ind}, is defined by

$$C_6^{\text{ind}} = \alpha_H \mu_{AH}^2 \quad (5)$$

where α_H is the H polarizability and μ_{AH} is the AH diatom dipolar moment. The parameters entering formulas 3 and 5 can be found in Table 1, and the C_6 parameters are collected in Table 2.

TABLE 1: Parameters Entering Formulas 3−6

	α (10^{-24} cm^3)[62−64]	n	μ (D)[65]	ω_e (cm^{-1})[66]	$\omega_e x_e$ (cm^{-1})[66]	r_e (Å)[66]
H_2	0.8023	2	−	4401.21	121.333	0.741
CH ($X\,^2\Pi$)	1.415	1	1.46	2858.5	63.02	1.12
NH ($X\,^3\Sigma^-$)	0.922	2	1.71	3282.2	78.3	1.0362
OH ($X\,^2\Pi$)	0.581	1	1.734	3737.76	84.88	0.969
SH ($X\,^2\Pi$)	1.728	1	1.0476	2711	59.9	1.34
H	0.667	1				
$C(^1D)$	0.816	2				
$N(^2D)$	0.538	3				
$O(^1D)$	0.323	2				
$S(^1D)$	1.153	2				

TABLE 2: C_6 Parameters Characterizing Each Reactant and Product Channel

	$C + H_2$	$S + H_2$	$O + H_2$
C_6 (eV·Å^6)	8.089	7.383	3.935
	CH + H	SH + H	OH + H	NH + H
ΔE_0(eV)	0.17	0.18	1.89	1.25
C_6^{disp} (eV·Å^6)	7.394	8.50	3.858	6.463
C_6^{ind} (eV·Å^6)	0.888	0.457	1.252	1.217
C_6 (eV·Å^6)	8.282	8.957	5.110	7.680

As the collision energies considered in this work are relatively small (no more than 0.165 eV), the entrance centrifugal barriers are expected to lie in almost isotropic regions of the PESs. For exit channels, due to the processes' exoergicity, this is much more questionable. Nevertheless, the isotropic assumption for fragment interactions is mandatory for implementation of PST which, as presented below, leads to an exceptionally simple and accurate determination of the state-resolved integral and differential cross sections.

Among all the atom−diatom systems studied here, interactions between $N(^2D)$ and H_2 cannot reasonably be approximated by eq 2. As a matter of fact, the NH_2 PES reveals a small potential energy barrier associated with a strong anisotropy in the entrance channel.[21] As a consequence, dynamics is governed by short-range forces that involve couplings between vibration, rotation, and translation motions. In this case, complex formation dynamics is estimated via the previously mentioned post-ADLOC model[38] (see Appendix A).

(3) Because of the deep potential energy well existing along the reaction path,[24] strong couplings take place between the AH_2 internal vibrational modes. As a result, intravibrational redistribution (IVR) is expected to lead to complete energy randomization on a time scale much shorter than the average time for AH_2 dissociation. This assumption associated with the preceding one (2) makes equally likely all final states available to the system, subject to conservations of total energy and total angular momentum.

(4) Internal fragment vibration is quantized whereas rotation and translation are treated classically.[32,33,43,44] Diatomic molecules are described as rigid-rotor anharmonic oscillators (RRAO) for which the vibrational energy levels are approximated by a Dunham expansion up to the second order,

$$E_v = hc\omega_e\left(v+\frac{1}{2}\right) - hc\omega_e x_e\left(v+\frac{1}{2}\right)^2 \qquad (6)$$

where the wavenumbers ω_e and $\omega_e x_e$ are collected in Table 1 for each diatom.

Considering assumptions (1)−(4), the state-resolved differential cross section (DCS) for reaction 1b can be evaluated by

$$\frac{d\sigma(v',j',\phi',E_c)}{d\omega} = \frac{1}{2\sin\phi'\,\mu E_c}\int_0^{J_{MAX}} P_{cap}(E_c,J)\,P_P(v',j',\phi',E',J)\,J\,dJ \qquad (7)$$

where E_c is the collision energy, J is the total angular momentum, μ is A−H_2 reduced mass, ϕ' is the center-of-mass scattering angle, $d\omega$ is the differential solid angle, and E' is the total excess energy with respect to the bottom of the product channel P. Given assumption 1 and 4, E' is defined by

$$E' = E_c + \Delta E_0 + E_{v=0} \qquad (8)$$

where ΔE_0 is the reaction exoergicity excluding the reactant and product zero point energies (ZPEs) (see Table 2) and $E_{v=0}$ is estimated via eq 6 with $v = 0$. The method for determining the maximum value J_{MAX} of J is presented in Appendix A. In eq 7, $P_{cap}(E_c,J)$ is the J-dependent probability for complex formation (opacity function), which can be estimated via the Langevin capture model[37] for the processes involving C, O, and S. Alternatively, $P_{cap}(E_c,J)$ is predicted via the previously mentioned post-ADLOC model for the reaction involving N(^{2}D). $P_P(v',j',\phi',E',J)$ is the probability that the intermediate complex dissociates producing the AH molecule in the (v', j') state, at total energy E' and total angular momentum J, the scattering angle being ϕ'. The latter probability is calculated, within the framework of PST,[32−36] as the ratio of the number $2\Omega_P(v',j,\phi',E',J)$ of product states consistent with the preceding conditions and the total number $\Omega_R(E,J)$ plus $2\Omega_P(E',J)$ of reactant and product states energetically accessible, subject to conservation of total angular momentum

$$P_P(v',j',\phi',E',J) = \frac{2\Omega_P(v',j',\phi',E',J)}{\Omega_R(E,J) + 2\Omega_P(E',J)} \qquad (9)$$

The factor 2 explicitly accounts for the degeneracy of channel P and E is the total excess energy with respect to the bottom of the reactant channel R, that is, $E = E_c + E_{v=0}$. The number of states Ω_i, entering eq 9, can be numerically estimated via Monte Carlo calculations[45] of phase space integrals.[46,47] These developments, presented in Appendix B, include a semiclassical treatment of tunneling through the centrifugal barriers.

The total differential cross section is recovered from eq 7 by integration over rotational angular momentum j' and summation over vibrational levels v',[48]

$$\frac{d\sigma(\phi',E_c)}{d\omega} = \sum_{v'=0}^{v'_{MAX}} \int_{j'=0}^{j'_{MAX}} \frac{d\sigma(v',j',\phi',E_c)}{d\omega}\,dj \qquad (10)$$

where v'_{MAX} is the maximal value of vibrational quantum number consistent with energy E' and the maximum value j'_{MAX} of the rotational angular momentum j' is calculated via eq 24 in Appendix B.

The state-resolved integral cross section is determined from eq 7 by integration with respect to the center-of-mass scattering angle ϕ':[49]

$$\sigma(v',j',E_c) = 2\pi\int_0^{\pi}\frac{d\sigma(v',j',\phi',E_c)}{d\omega}\sin\phi'\,d\phi' \qquad (11)$$

3. Results and Discussion

The PST approach is compared to exact time-independent quantum scattering calculations and either the CCS or WPS models depending on the availability of data in the literature. As both the CCS and WPS models rely on the same statistical assumption for the intermediate complex and treat exactly the entrance/exit channels quantum dynamics, they are assumed to give identical results. These methods will be referred as "exact statistical models" in the following. Extensive comparisons between the CCS model and exact quantum scattering calculations have been performed for the processes involving N(^{2}D) and O(^{1}D),[19] which are associated with significant exoergicities. For the much less exoergic reactions involving C(^{1}D) and S(^{1}D), comparisons are less extensive. Nevertheless, the statistical assumption is a priori more justified as excess energies in the product channels are smaller and, as a consequence, complex resonance states are longer-lived. For these latter reactions, the agreement between exact quantum scattering calculations and the CCS model, for DCSs, is almost perfect (see for example Figures 4 and 8 in ref 24).

C(^{1}D) + H_2(v=0, j=0) → CH(X^2 Π, v', j') + H. This reaction proceeds through a 4.29 eV deep well relative to the reactants and is associated with a 0.17 eV exoergicity (excluding ZPEs). State-resolved ICS and DCS have been predicted by the exact quantum scattering calculations of Banares et al.[7] at 80 meV collision energy. Besides, the CCS[24] and WPS[26] have been applied to estimate respectively the total DCS and the state-resolved ICS. The upper panel of Figure 1 displays the CH(v'=0) rotationally resolved ICSs resulting from exact quantum scattring calculations, WPS and PST models. It has to be noticed that, at this collision energy, the CH(v'=1) population is almost negligible. The total DCSs determined by exact quantum scattering calculations and the CCS and PST models are displayed in the lower panel of Figure 1. The agreement between quantum calculations and the CCS model is very good. The PST approach leads to a fair agreement with both previous methods for ϕ' values ranging from 20° to 160°. However, the strong polarization in the first and last 20° is not reproduced.

S(^{1}D) + H_2(v=0, j=0) → SH(X ^{2}Π, v', j') + H. As far as energetics is concerned, this process is similar to the previous one as the PES involves a 4.23 eV deep well relative to the reactants and is exothermic by about 0.18 eV. Exact quantum scattering calculations have been performed by Launay and coworkers.[10,16] In addition, for a collision energy of 97 meV, the WPS[12] model has been applied to predict the state-resolved DCSs and ICSs.[12] The comparison between these exact approaches and PST is displayed in Figure 2. As in the case of the reaction involving C(^{1}D), the agreement is rather good but the strong polarization exhibited in the total DCSs is not accounted for. However, it has to be noticed that such a disagreement also exists between quantum scattering calculations and the WPS model at $\phi' = 0°$ (for $v' = 0$).

O(^{1}D) + H_2(v=0, j=0) → OH(X ^{2}Π, v', j') + H. This reaction involves a 7.29 eV deep well relative to the reactants

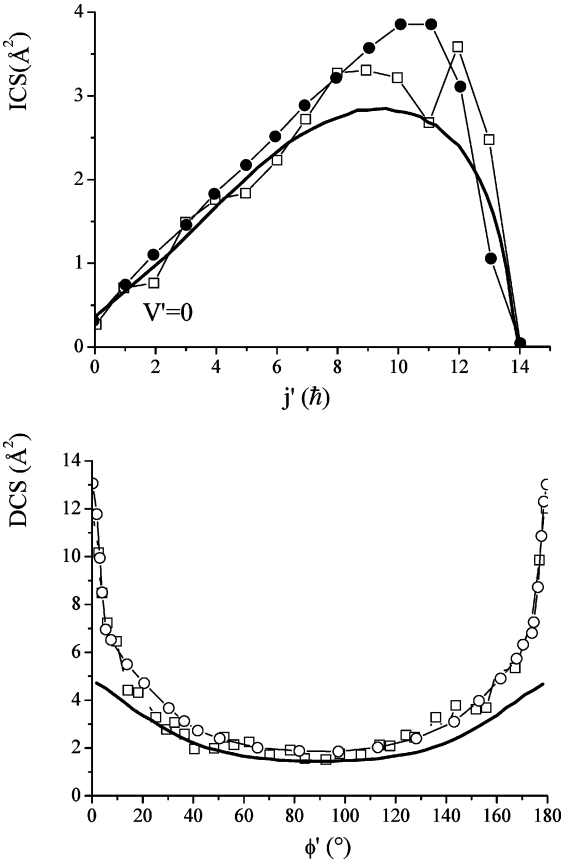

Figure 1. $v' = 0$ state-resolved integral cross section (upper panel) and total differential cross section (lower panel) for the reaction $C(^1D) + H_2(v = j = 0) \rightarrow CH(X\ ^2\Pi) + H$ at 80 meV collision energy: (−□−) quantum scattering calculations; (−○−) CCS model; (−●−) WPS model; (bold line) present PST approach.

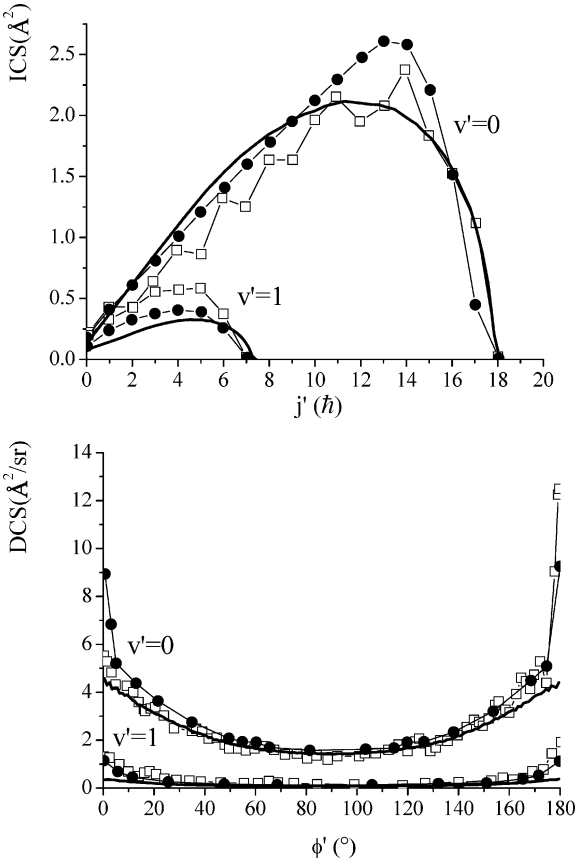

Figure 2. State-resolved integral cross section (upper panel) and total differential cross section (lower panel) for the reaction $S(^1D) + H_2(v = j = 0) \rightarrow SH(X\ ^2\Pi) + H$ at 97 meV collision energy: (−□−) quantum scattering calculations; (−●−) WPS model; (bold line) present PST approach.

and a significant exoergicity of 1.89 eV. Extensive comparisons between exact quantum scattering calculations[9] and the CCS[19,24] and PST models are displayed in Figures 3 and 4. Vibrationally resolved ICS and total DCS are presented for various collision energies in Figure 3. State-resolved ICSs, corresponding to 100 meV collision energy, are shown in Figure 4. Again, except the backward/forward polarizations appearing in the quantum and CCS total DCSs, the results of the PST approach are very satisfactory.

$N(^1D) + H_2(v=0, j=0) \rightarrow NH(X\ ^3\Sigma^-, v', j') + H$. This reaction involves a deep well of 5.48 eV relative to the reactants and a significant exoergicity of 1.25 eV. However, this process differs from the three previous ones as it involves a small potential energy barrier and a strong anisotropy in the $N+H_2$ channel. Accordingly, the PST approach is slightly modified in that the complex formation opacity function $P_{cap}(E_c,J)$ is estimated via the recently developed post-ADLOC model. Nevertheless, as indicated in Appendix B, the probability $P_P(v',j',\phi',E',J)$ can be calculated via PST, neglecting the term $\Omega_R(E,J)$ in eq 9. Figure 5 displays the NH vibrationally resolved ICSs resulting from exact quantum scattering and the CCS and modified-PST models for various collision energies. Total DCSs are also presented. In addition, to point up the close agreement between the CCS and modified-PST models in this case, the state-resolved ICSs corresponding to 165 meV collision energy are displayed in Figure 6.

As illustrated by Figures 1−6, the overall agreement between PST and exact quantum scattering calculations is unexpectedly good. Given the excellent results of both the CCS and WPS models, the statistical assumption for the intermediate complex was expected to be quite reliable. Nevertheless, the basic hypothesis (2) of the PST approach seems also to be valid. This semiclassical PST model (without tunneling correction) has already led to a rather good description of the product translational energy distributions for the NO_2 and C_2O unimolecular dissociation.[50] Other applications of quantized PST have also been performed in the past.[51−53] However, to our knowledge, this work is the first such systematic and severe test of PST for such detailed observables on a class of bimolecular triatomic reactions. It has to be noticed that ICSs and DCSs are computed without any normalization factor as it is often the case for product energy distributions.

For barrierless processes, here those involving $C(^1D)$, $O(^1D)$, and $S(^1D)$, the strength of the PST approach stems from the fact that no information on the ab initio potential energy surfaces is required. For the $N + H_2$ reaction, very little information on the PES is needed.[38] Therefore, such a method gives trustworthy estimates of experimental observables without involving cumbersome electronic structure and dynamical simulations.

However, the agreement between the PST approach and the exact statistical and dynamical methods is not perfect. The sharp forward/backward peaks appearing systematically in the state-resolved or total DCSs are not predicted. As mentioned earlier, such polarizations, which are not reproduced by QCT and not seen in the experiments,[54] have been ascribed to tunneling through centrifugal barriers lying in the long-range regions of the PESs. In our version of PST, tunneling is approximately accounted for (see Appendixes A and B) but its effect on the predicted ICSs and DCSs is found almost negligible. The discrepancies between PST and other approaches are then

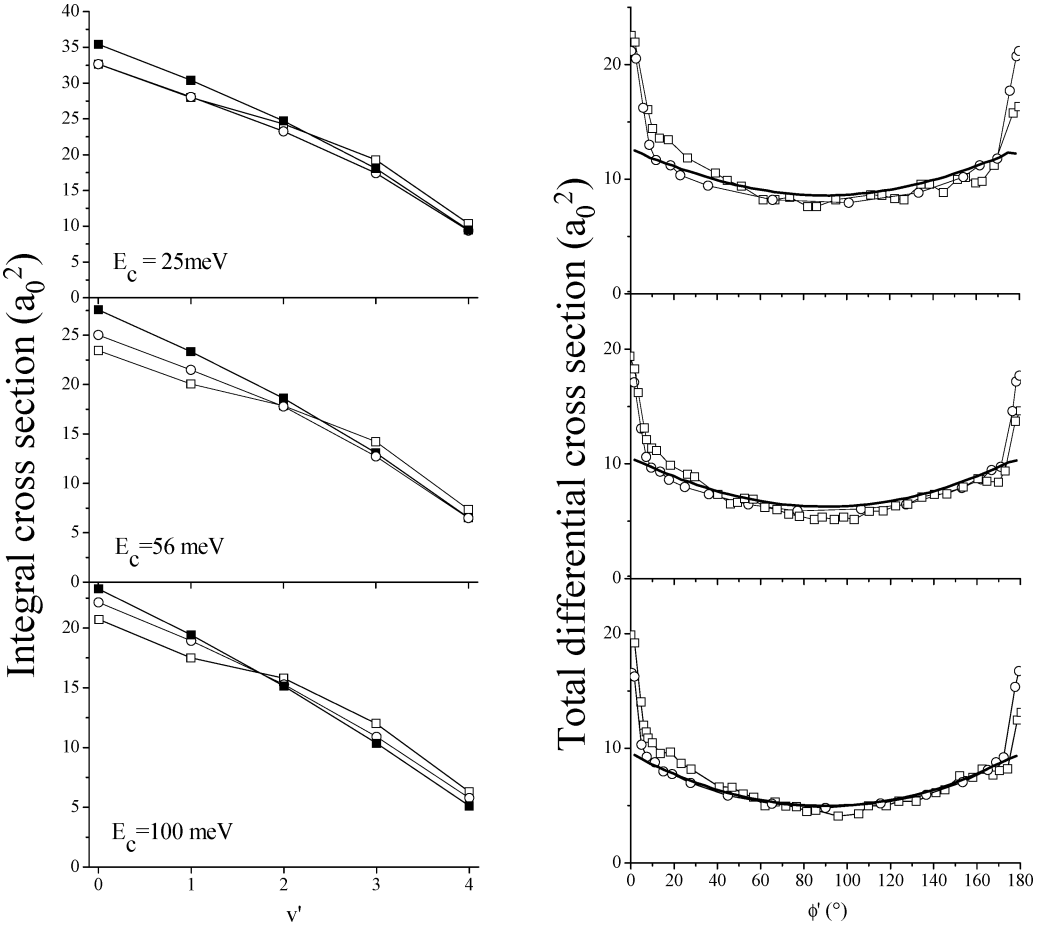

Figure 3. Vibrational integral cross section (left) and total differential cross section (right) for the reaction $O(^1D) + H_2(v = j = 0) \rightarrow OH(X\ ^2\Pi) + H$ at three collision energies indicated on the left plots: (−■−, left, and bold line, right) present PST approach; (−□−) quantum scattering calculations; (−○−) CCS model.

presumably related to the isotropic approximation for fragment interactions. Work is in progress to understand this divergence.

A few years ago, Chang and Lin[55] used both PST and variational RRKM theory in order to predict the S + H_2 (HD, D_2) isotopic reaction rate constants. The predicted cross section isotope ordering was found in disagreement with the molecular beam experiments of Lee and Liu.[56] Consequently, the authors concluded that their results were "not in supportive of a long-lived complex". Nevertheless, Rackham et al. recently proved that the statistical assumption for the intermediate complex was justified and argued that the previous PST and RRKM approaches were not accurate enough. In particular, they suggested that the discrepancies could originate from the isotropic approximation for fragment interactions and the lack of tunneling in capture dynamics. The quality of our PST description of state-resolved ICSs and DCSs is not in line with this latter suggestion. Furthermore, recent theoretical studies based on the statistical wave packet based model[12] and QCT/QM calculations[29] have led to results in fair agreement with those of Chang and Lin thus questioning experiment.

Our results suggest that the PST-based model comprises the essential physical ingredients of atom−diatom insertion dynamics. This approach, which is straightforward to implement with respect to the exact ones, is thus a valuable tool to characterize experimental data.

Last but not least, several theoretical studies, based on PST[32−36] (and more generally transition-state theory[57]) have been recently developed in order to rationalize dynamics of complex-forming reaction.[18,58] The relevance of such studies, that have evidenced simple key parameters influencing the shape of product state distributions, is greatly strengthened by the present results.

4. Conclusion

A PST approach has been developed in order to predict state-resolved integral and differential cross sections for atom−diatom insertion reactions of the type A + $H_2 \rightarrow AH_2 \rightarrow$ AH + H with A = $C(^1D)$, $S(^1D)$, $O(^1D)$, and $N(^2D)$. This model is based on three main assumptions: (i) fast energy randomization among internal degrees of freedom of the AH_2 intermediate complex (statistical assumption), (ii) quantization of the diatomic vibration motion and classical treatment of the rotation and translation motions in the entrance/exit channels, and (iii) approximation of fragment interactions in the reactant/product channels by long-range van der Waals interactions (except for the N + H_2 channel, see text). Given the simplicity of PST, the predicted state-resolved integral and differential cross sections are found in quite good agreement with exact quantum dynamics scattering calculations and exact quantum statistical models. These results highlight the relevancy of such a simple statistical approach in describing complex-forming reaction dynamics. This work is, to our knowledge, the first such systematic comparison of PST predictions with accurate quantum scattering and quantum statistical calculations.

Appendix A

Coordinates. The reactant atom−diatom system is described within the following set of 12 canonical coordinates:[43] the total

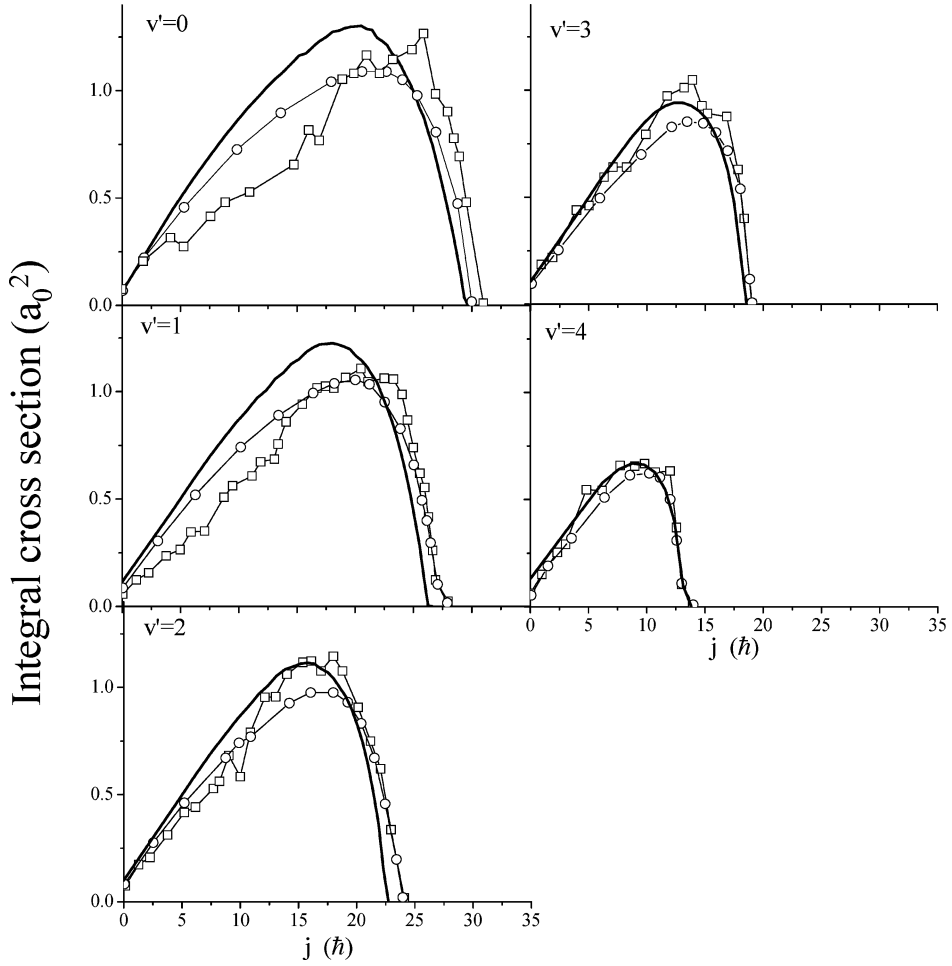

Figure 4. State-resolved integral cross section for the reaction $O(^1D) + H_2(v = j = 0) \rightarrow OH(X\ ^2\Pi) + H$ at 100 meV collision energy, with the OH vibrational quantum number indicated on each plot: (bold line) present PST approach; (−□−) quantum scattering calculations; (−○−) CCS model.

angular momentum J, its space fixed component J_z, the orbital angular momentum L, the diatom rotational angular momentum j, their respective conjugate angles α, β, α_L, α_j, the distance R between the atom and the diatom center-of-mass, the diatom bound distance r and their respective conjugate momenta P_R and p_r. Furthermore, μ and m are respectively the reactant atom−diatom and diatom reduced masses and r_e is the diatom equilibrium distance. The product atom−diatom system is defined by an equivalent set of primed coordinates J', J'_z, L', j', α', β', α'_L, α'_j, R', r', P'_R, p'_r, μ', m', r'_e.

Capture Probability $P_{cap}(E_c,J)$. The probability for intermediate complex formation is evaluated using the Langevin capture model.[37] As mentioned above, j is neglected so that $J = L$. Within the framework of the previous model, all atom−diatom systems colliding with an energy E_c and involving a total angular momentum lower than the maximum value, J^{Cl}_{MAX}, lead to formation of the AH_2 complex with unit probability:

$$P_{cap}(E_c,J) = 1 \quad \text{for} \quad J < J^{Cl}_{MAX} \tag{12}$$

Approximating the interaction potential energy by eq 2, the maximum value of total angular momentum consistent with capture is given by[18]

$$J^{Cl}_{MAX} = (3\mu)^{1/2}(2C_6)^{1/6}(E_c)^{1/3} \tag{13}$$

where C_6 is the potential parameter entering eq 2.

For $J > J^{Cl}_{MAX}$, complex formation is classically forbidden as collision energy E_c is lower than the top of the centrifugal barrier. Nevertheless, one-dimensional tunneling through this effective potential barrier can be estimated using the WKB semiclassical approximation,[59]

$$P_{cap}(E_c,J) = \frac{1}{1 + e^{2\theta}} \tag{14}$$

where θ is the phase integral defined by

$$\theta = \frac{2\pi}{h}\int_{R_-}^{R_+}\sqrt{2\mu(V_{eff}(R) - E_c)}\,dR \tag{15}$$

calculated through the effective potential,

$$V_{eff}(R) = \frac{J^2}{2\mu R^2} + V(R) \tag{16}$$

where $V(R)$ is the atom−diatom interaction potential. R_+ and R_- are defined by the integrand condition of existence. The maximum value J_{MAX} of J consistent with capture and including tunneling is here arbitrarily defined by $P_{cap}(E,J_{MAX}) = 10^{-3}$.[60] It has to be noticed that $P_{cap}(E,J)$ is overestimated, for J tending to J^{Cl}_{MAX} by lower values, as quantum reflection[61] is not taken into account. This way of determining capture probability can be applied to the processes characterized by barrierless entrance channels, namely, those involving $O(^1D)$, $S(^1D)$, and $C(^1D)$. In

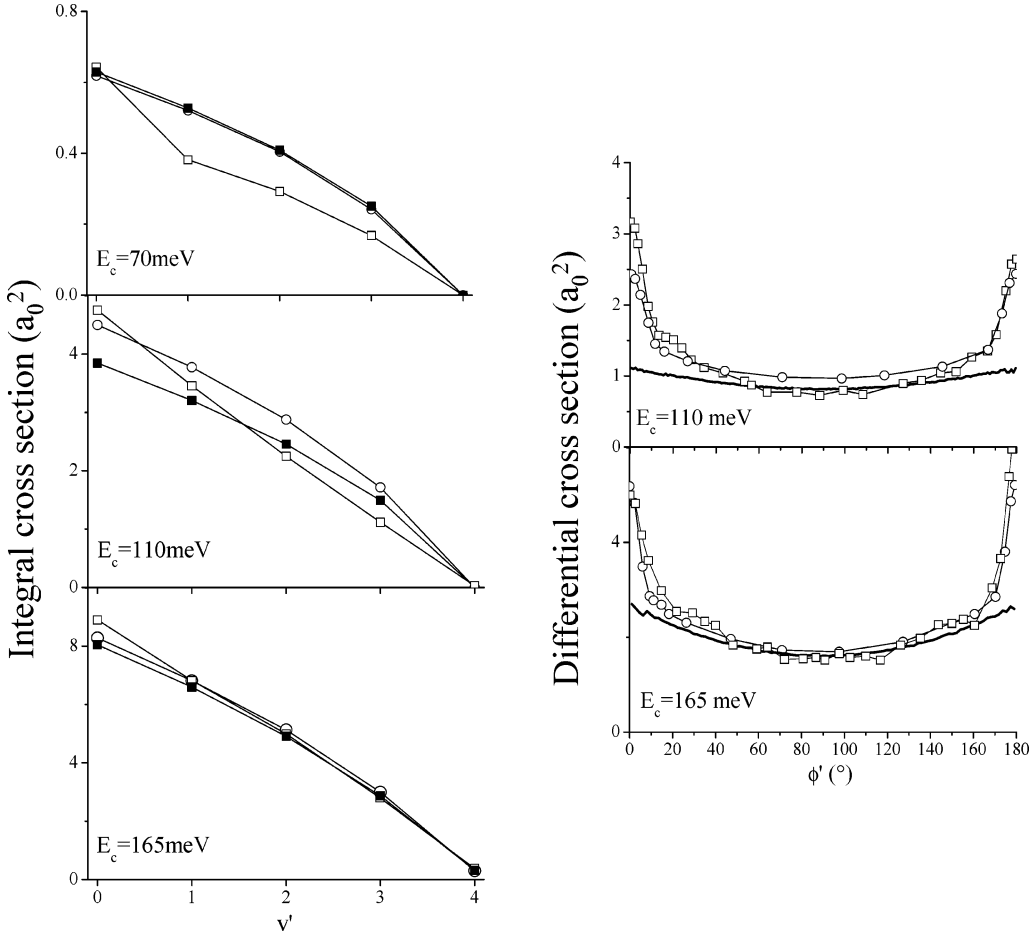

Figure 5. Vibrational integral cross section (left) and total differential cross section (right) for the reaction $N(^2D) + H_2(v = j = 0) \rightarrow NH(X\ ^3\Sigma^-) + H$, with the collision energies indicated on each plot: (−■−, left, and bold line, right) present modified-PST approach; (−□−) quantum scattering calculations; (−○−) CCS model.

contrast, as mentioned in part 2, it is inappropriate for the prediction of the NH_2-complex formation probability. Instead, the post-ADLOC model must be employed, which takes into account fragment reorientation during approach as well as tunneling (formulas 4.1−4.3 in ref 38).

Appendix B

Calculation of $P_P(v',j',\phi',E',J)$. As stated in part 2, the PST calculation of the probability that the intermediate complex leads to the AH molecule in the (v', j') state, at total energy E', total angular momentum J, and the scattering angle being ϕ', requires the knowledge of the number of product states, $2\Omega_P(v',j',\phi',E',J)$, consistent with v', j', and ϕ', and the total number of reactant and product states energetically available under conservation of total angular momentum, respectively $\Omega_R(E,J)$ and $2\Omega_P(E',J)$ (eq 9).

$\Omega_P(E',J)$. The total number of product states $2\Omega_P(E',J)$ can be estimated as follows:

$$\Omega_P(E',J) = \sum_{v'=0}^{v'_{MAX}} \Omega_P^{ROT}(v',E',J) \tag{17}$$

where $\Omega_P^{ROT}(v',E',J)$ is the number of rotational and orbital states such that the diatom rotational energy is lower than $E' - E'_{v'}$ where $E'_{v'}$ is the internal vibration energy. v'_{MAX} is the maximal value of the vibrational quantum number v' consistent with E'. As rotational and orbital degrees of freedom are treated classically, $\Omega_P^{ROT}(v',E',J)$ is estimated via semi-classical quantization of the corresponding phase space volume, that is,

$$\Omega_P^{ROT}(v',E',J) = \int \frac{d\Gamma}{h^4} \prod_{i=1}^{5} \Delta_i \tag{18}$$

where $d\Gamma$ is the differential phase space volume associated to rotational and orbital degrees of freedom, $d\Gamma$ (dJ', dJ'_z, dL', dj', $d\alpha'$, $d\beta'$, $d\alpha'_L$, $d\alpha'_j$). The Δ_is ($i = 1-5$) define the constraints limiting the integration domain (δ and θ are the Dirac and Heaviside functions, respectively):

$$\Delta_1 = \delta(J' - J) \tag{19}$$

$$\Delta_2 = \theta(j'_{MAX} - j') \tag{20}$$

$$\Delta_3 = \theta(L'_{MAX} - L') \tag{21}$$

$$\Delta_4 = \theta(J - |L' - j'|)\, \theta(L' + j' - J) \tag{22}$$

$$\Delta_5 = P(v',j',L') \tag{23}$$

Δ_1 ensures that $J' = J$, Δ_2 and Δ_3 restrict the domain of integration with respect to j' and L' up to the maximal value energetically available, Δ_4 imposes the triangular inequality resulting from $J = L' + j'$, and Δ_5 is a probability associated to each state whether it is classically accessible from the intermediate complex or not. Its determination is detailed below.

The maximum value of the product diatom angular momentum is given by

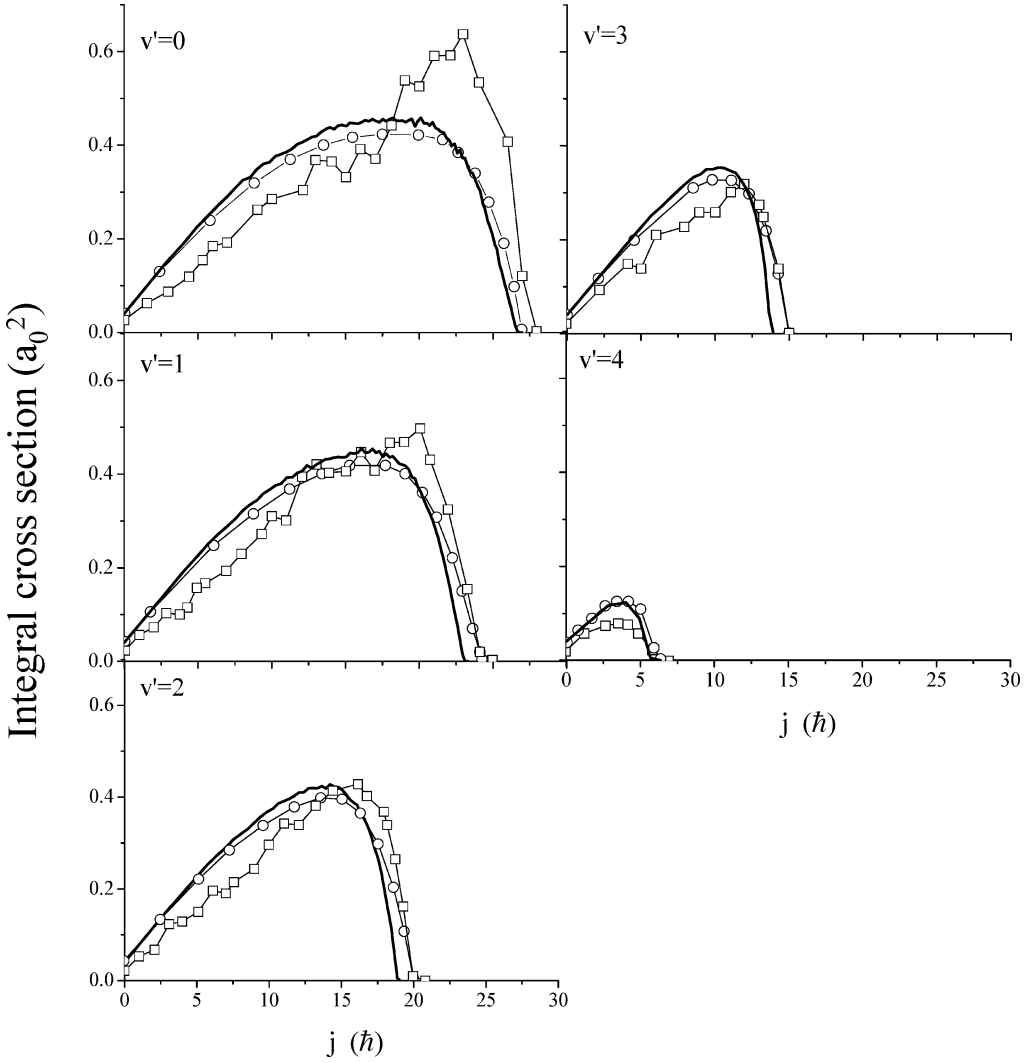

Figure 6. State-resolved integral cross section for the reaction $N(^2D) + H_2(v = j = 0) \rightarrow NH(X\ ^3\Sigma^-) + H$ at 165 meV collision energy, with the NH vibrational quantum number indicated on each plot: (bold line) present modified-PST approach; (−□−) quantum scattering calculations; (−○−) CCS model.

$$j'_{MAX} = \sqrt{2m'r'_e{}^2(E' - E'_{v'})} \tag{24}$$

For given v' and j', the translational energy in the products is

$$E'_T = E' - E'_{v'} - \frac{j'^2}{2m'r'_e{}^2} \tag{25}$$

so that the maximum value of orbital angular momentum, consistent with formation of products from the intermediate complex, is given by (equivalently to eq 13)

$$L'^{Cl}_{MAX} = (3\mu')^{1/2}(2C'_6)^{1/6}(E'_T)^{1/3} \tag{26}$$

where C'_6 is the potential energy parameter of eq 2. However, as products may be formed by tunneling through the exit centrifugal barrier, L' may be greater than L'^{Cl}_{MAX} but is limited in any case, by total angular momentum conservation, to

$$L'_{MAX} = J + j'_{MAX} \tag{27}$$

In analogy with the method used to include tunneling into the Langevin model (see above), the probability $P(v',j',L')$ associated with a product state (v', j', L') can be predicted using eqs 12−16, replacing J by L' and E_c by E'_T (eq 25) and using the parameters corresponding to the P product channel.

Integrating with respect to α', β', $\alpha_{L'}$, $\alpha_{j'}$, J', and J'_z and expressing the momenta in $\hbar$ units, eq 18 can be rewritten as

$$\Omega_P^{ROT}(v',E',J) = 2J\int dj'\, dL' \prod_{i=2}^{5}\Delta_i \tag{28}$$

The Monte Carlo integration method[45] can be further used to integrate this expression with respect to j' and L'. N points of coordinates (j', L') are randomly chosen such that $L' < L'_{MAX}$, and $j' < j'_{MAX}$ (constraints Δ_2 and Δ_3). For the M points satisfying constraints Δ_4, $P(v',j',L')$ is then estimated such that eq 28 reduces to

$$\Omega_P^{ROT}(v',E',J) = 2JL'_{MAX}j'_{MAX}\frac{\sum_M P(v',j',L')}{N} \tag{29}$$

$\Omega_P(E',J)$ is then recovered by summing $\Omega_P^{ROT}(v',E',J)$ over the available vibrational levels through eq 17.

$\Omega_R(E,J)$. $\Omega_R(E,J)$ can be estimated in a similar way as $\Omega_P(E',J)$, i.e., using eqs 17−29 and replacing all the primed coordinates and parameters by the equivalent unprimed ones characterizing the R reactant channel. However, for the process

involving $N(^2D)$, PST cannot be used as reactant channel dynamics is governed by short-range forces. Alternatively, the total number of reactant states could be predicted by semiclassical quantization of the phase space flux through the tight transition state (hypersurface defined by the position of the barrier along the reaction path). Nevertheless, due to the process exoergicity and the low value collision energies considered in this work (lower than 0.165 meV), $\Omega_R(E,J)$ is negligible with respect to $\Omega_P(E',J)$ so that its calculation is unnecessary.

$\Omega_P(v',j',\phi',E',J)$. $\Omega_P(v',j',\phi',E',J)$ can be evaluated in a similar way as $\Omega_P^{ROT}(v',E',J)$ with additional constraints on the j' and ϕ'coordinates. Let us divide the range $[0, j'_{MAX}]$ into N_j intervals $I_i^j = [i\cdot j'_{MAX}/N_j; (i+1)\cdot j'_{MAX}/N_j]$, i varying from 0 to $N_j - 1$ and j'_{MAX} being the maximal value of the product diatom rotational momentum (eq 24). Similarly, concerning the ϕ' variable, let us divide the range $[0, \pi]$ into N_ϕ intervals $I_i^\phi = [i\cdot\pi/N_\phi; (i+1)\cdot\pi/N_\phi]$, i varying from 0 to $N_\phi - 1$. The number of product states corresponding to v', E', J with j' belonging to the interval I_i^j (i.e. $j' \sim (i+0.5)\cdot j'_{MAX}/N_j$) and ϕ' belonging to the interval I_i^ϕ (i.e. $\phi' \sim (i+0.5)\cdot\pi/N_\phi$) can be calculated via eq 18 adding the two following extra constraints:

$$\Delta_6 = \theta\left(j' - \frac{i\cdot j'_{MAX}}{N_j}\right)\theta\left(\frac{(i+1)\cdot j'_{MAX}}{N_j} - j'\right) \qquad (30)$$

$$\Delta_7 = \theta\left(\frac{\phi' - i\cdot\pi}{N_\phi}\right)\theta\left(\frac{\phi' - (i+1)\cdot\pi}{N_\phi}\right) \qquad (31)$$

The relationship linking the scattering angle ϕ' to the canonical coordinates (J, L', j', α', α'_L), which can be deduced from the developments of ref 43, is given by

$$\cos\phi' = \cos\alpha'_L\cdot\sin\alpha' + \cos\alpha'\cdot\sin\alpha'_L\cos\left(\frac{J^2 + L'^2 - j'^2}{2L'J}\right) \qquad (32)$$

N points of coordinates (j', L') are randomly chosen such that $L' < L'_{MAX}$, and $j' < j'_{MAX}$. α' and α'_L are randomly chosen in the interval $[0;2\pi]$, and ϕ' is calculated from eq 32. For the M points satisfying constraints Δ_4, Δ_6, and Δ_7, Δ_5 is evaluated and $\Omega_P(v',j',\phi',E',J)$ is recovered using eq 29.

References and Notes

(1) Casavecchia, P. *Rep. Prog. Phys.* **2000**, *63*, 355.
(2) Liu, K. *Annu. Rev. Phys. Chem.* **2001**, *52*, 139.
(3) Bergeat, A.; Cartechini, L.; Balucani, N.; Capozza, G.; Phillips, L. F.; Casavecchia, P.; Volpi, G. G.; Bonnet, L.; Rayez, J. C. *Chem. Phys. Lett.* **2000**, *327*, 197.
(4) Balucani, N.; Cartechini, L.; Capozza, G.; Segoloni, E.; Casavecchia, P.; Volpi, G. G.; Javier Aoiz, F.; Banares, L.; Honvault, P.; Launay, J.-M. *Phys. Rev. Lett.* **2002**, *89*, 013201/1.
(5) Aoiz, F. J.; Banares, L.; Castillo, J. F.; Herrero, V. J.; Martinez-Haya, B.; Honvault, P.; Launay, J. M.; Liu, X.; Lin, J. J.; Harich, S. A.; Wang, C. C.; Yang, X. *J. Chem. Phys.* **2002**, *116*, 10692.
(6) Lee, S. H.; Liu, K. *Appl. Phys. B: Lasers Opt.* **2000**, *71*, 627.
(7) Banares, L.; Aoiz, F. J.; Honvault, P.; Bussery-Honvault, B.; Launay, J. M. *J. Chem. Phys.* **2003**, *118*, 565.
(8) Honvault, P.; Launay, J. M. *J. Chem. Phys.* **1999**, *111*, 6665.
(9) Honvault, P.; Launay, J. M. *J. Chem. Phys.* **2001**, *114*.
(10) Honvault, P.; Launay, J. M. *Chem. Phys. Lett.* **2003**, *370*, 371.
(11) Lin, S. Y.; Guo, H. *J. Phys. Chem. A* **2004**, *108*, 2141.
(12) Lin, S. Y.; Guo, H. *J. Chem. Phys.* **2005**, *122*, 074304/1.
(13) Mouret, L.; Launay, J.-M.; Terao-Dunseath, M.; Dunseath, K. *Phys. Chem. Chem. Phys.* **2004**, *6*, 4105.
(14) Defazio, P.; Petrongolo, C. *J. Theor. Comput. Chem.* **2003**, *2*, 547.
(15) Hankel, M.; Balint-Kurti, G. G.; Gray, S. K. *J. Phys. Chem. A* **2001**, *105*, 2330.
(16) Banares, L.; Aoiz, F. J.; Honvault, P.; Launay, J. M. *J. Phys. Chem. A* **2004**, *108*, 1616.
(17) Lin, S. Y.; Guo, H.; Farantos, S. C. *J. Chem. Phys.* **2005**, *122*, 124308.
(18) Bonnet, L.; Rayez, J. C. *Phys. Chem. Chem. Phys.* **1999**, *1*, 2383.
(19) Rackham, E. J.; Huarte-Larranaga, F.; Manolopoulos, D. E. *Chem. Phys. Lett.* **2001**, *343*, 356.
(20) Bussery-Honvault, B.; Honvault, P.; Launay, J. M. *J. Chem. Phys.* **2001**, *115*, 10701.
(21) Pederson, L. A.; Schatz, G. C.; Ho, T. S.; Hollebeek, T.; Rabitz, H.; Harding, L. B.; Lendvay, G. *J. Chem. Phys.* **1999**, *110*.
(22) Dobbyn, A. J.; Knowles, P. J. *Mol. Phys.* **1997**, *91*, 1107.
(23) Ho, T.-S.; Hollebeek, T.; Rabitz, H.; Chao, S. D.; Skodje, R. T.; Zyubin, A. S.; Mebel, A. M. *J. Chem. Phys.* **2002**, *116*, 4124.
(24) Rackham, E. J.; Gonzalez-Lezana, T.; Manolopoulos, D. E. *J. Chem. Phys.* **2003**, *119*, 12895.
(25) Alexander, M. H.; Rackham, E. J.; Manolopoulos, D. E. *J. Chem. Phys.* **2004**, *121*, 5221.
(26) Lin, S. Y.; Guo, H. *J. Chem. Phys.* **2004**, *120*, 9907.
(27) Lin, S. Y.; Guo, H. *J. Phys. Chem. A* **2004**, *108*, 10066.
(28) Balucani, N.; Capozza, G.; Cartechini, L.; Bergeat, A.; Bobbenkamp, R.; Casavecchia, P.; Javier Aoiz, F.; Banares, L.; Honvault, P.; Bussery-Honvault, B.; Launay, J.-M. *Phys. Chem. Chem. Phys.* **2004**, *6*, 4957.
(29) Banares, L.; Castillo, J. F.; Honvault, P.; Launay, J. M. *Phys. Chem. Chem. Phys.* **2005**, *7*, 627.
(30) Bonnet, L.; Rayez, J. C. *Chem. Phys. Lett.* **1997**, *277*, 183.
(31) Bonnet, L.; Rayez, J.-C. *Chem. Phys. Lett.* **2004**, *397*, 106.
(32) Light, J. C. *J. Chem. Phys.* **1964**, *40*, 3221.
(33) Pechukas, P.; Light, J. C. *J. Chem. Phys.* **1965**, *42*, 3281.
(34) Light, J. C. *Discuss. Faraday Soc.* **1967**, *44*, 14.
(35) Nikitin, E. E. *Theory of elementary Atomic and Molecular processes in Gases*; Clarendon: Oxford, 1974.
(36) Keck, J. C. *J. Chem. Phys.* **1958**, 410.
(37) Langevin, P. *Ann. Chim. Phys.* **1905**, *5*, 245.
(38) Larregaray, P.; Bonnet, L.; Rayez, J. C. *Phys. Chem. Chem. Phys.* **2002**, *4*, 1571.
(39) Smith, I. W. M. *J. Chem. Educ.* **1982**, *59*, 9.
(40) Bonnet, L.; Rayez, J. C. *Chem. Phys.* **1995**, *201*, 203.
(41) Given the collision energies considered in this work, much larger than in typical ultracold processes, the anisotropic quadruopole−quadrupole interaction existing in the entrance channels is expected to play a minor role. The interaction potential between reactants becomes significant at interfragment separations for which the quadrupole−quadrupole interaction is negligible with respect to the dispersion one (∼3 to 4 Å). The agreement between the PST total cross sections and the quantum ones, computed using the ab initio PES, justifies a posteriori this approximation.
(42) Hirschfelder, J. O.; Curtiss, C. F.; Bird, R. B. *Molecular Theory of Gases and Liquids*; Wiley: New York, 1954.
(43) Wardlaw, D. M.; Marcus, R. A. *J. Chem. Phys.* **1985**, *83*, 3462.
(44) It has to be noted that Pechukas and Light originally proposed both quantized and classical versions of PST (ref 33).
(45) Nougier, J. P. *Méthodes de Calcul Numérique*; Masson: Paris, 1983.
(46) Chesnavich, W. J.; Bowers, M. T. *J. Am. Chem. Soc.* **1976**, *98*, 8301.
(47) Bonnet, L.; Rayez, J. C.; Casavecchia, P. *Phys. Chem. Chem. Phys.* **2000**, *2*, 741.
(48) In practice, the integral of eq 10 can be calculated in the same way as eq 7, i.e., using eqs 12−32 of Appendixes A and B, excluding constraint Δ_6 (eq 30).
(49) In practice, eq 11 can be calculated using eqs 12−32 of Appendixes A and B excluding constraint Δ_7 (eq 31).
(50) Bonnet, L.; Rayez, J. C. *Chem. Phys. Lett.* **1998**, *296*, 19.
(51) Truhlar, D. G. *J. Chem. Phys.* **1969**, *51*, 4617.
(52) Truhlar, D. G.; Kupperman, A. *J. Phys. Chem.* **1969**, *73*, 1722.
(53) Truhlar, D. G. *J. Chem. Phys.* **1971**, *56*, 1481.
(54) Balucani, N.; et al. *J. Chem. Phys. 122*, 234309.
(55) Chang, A. H. H.; Lin, S. H. *Chem. Phys. Lett.* **2000**, *320*, 161.
(56) Lee, S.-H.; Liu, K. *Chem. Phys. Lett.* **1998**, *290*, 323.
(57) Truhlar, D. G.; Garret, B. C.; Klippenstein, S. J. *J. Phys. Chem.* **1996**, *100*, 12771.
(58) Larregaray, P.; Bonnet, L.; Rayez, J. C. *J. Chem. Phys.* **2001**, *114*, 3349.
(59) Child, M. S. *Semiclassical Mechanics with Molecular Applications*; Clarendon Press: Oxford, 1991.
(60) The results are insensitive to the number chosen provided that it is significantly lower than one.
(61) Pilling, M. J.; I. W. M., S. *Modern Gas Kinetics*; Blackwell Scientific Publications: Oxford, 1987.
(62) Miller, T. M.; Bederson, B. *Adv. At. Mol. Phys.* **1977**, *13*.
(63) Bridge, N. J.; Buckingham, A. D. *Proc. R. Soc.* **1966**, *A295*, 334.
(64) Gray, S. K.; Goldfield, E. M.; Schatz, G. C.; Balint-Kurti, G. G. *Phys. Chem. Chem. Phys.* **1999**, *1*, 1141.
(65) Nelson, R. D.; Lide, D. R.; Maryott, A. A. *Natl. Stand. Ref. Data Ser. (U.S., Natl. Bur. Stand.)* **1967**, *10*.
(66) *NIST Standard Reference Database Number 69*, March 2003 release.